






The MSC Prosthetic Hand: Rapid, Powerful, and Intuitive

Younggeol Cho , Yeongseok Lee , *Graduate Student Member, IEEE*, Pyungkang Kim ,
Seokhwan Jeong , and Kyung-Soo Kim , *Member, IEEE*

Abstract—Amputees suffer from the weight, insufficient power, and uncomfortable control methods of their prostheses. Recent studies have introduced many ideas for both hardware and software to tackle these problems. In this letter, the authors introduce a preliminary platform of a robotic prosthetic hand system called the MSC hand that integrates effective mechanical mechanisms and intuitive control methods. The hand adopts mode-switchable twisted string actuators to provide a wide range of grasping speed (closing speed of 0.8 s) and grasping force (pinch force of 45 N) with a light weight of 390 g. All the fingers and the thumb flex and extend actively, and the thumb is also able to abduct and adduct passively. The active fingers are controlled by surface electromyographic signals, and a learning-based neurophysiologic model is used to estimate human intention for each finger. The model provides independent intentions for each finger, so the simultaneous and proportional control of multiple fingers is possible in real time. The performance of the MSC hand was verified through standardized experiments such as online simulation and the box and block test. In addition, a demonstration of gripping various objects was performed. The results showed rapid and precise gripping and intuitive control over the tasks.

Index Terms—Prosthetic hand, twisted string actuator (TSA), electromyography (EMG), intention estimation.

I. INTRODUCTION

IN RECENT decades, the rapid improvement in 3D-printing, actuator, and sensor technologies has allowed mesoscale fabrication and design, facilitating various small-to-medium-sized robotic systems such as robotic hands and grippers. Robotically driven prosthetic hand is an emerging application, and many prototypes and commercial products have been developed and released to improve the quality of life for people who have

experienced amputation [1]–[3]. While multiple grasping motions and interfaces have been implemented in robotic prosthetic systems, it has been reported that most amputees still prefer conventional aesthetic prostheses due to the limited outputs, dexterity, difficulty of control, and cost of such systems [4].

Previous research suggested that prosthetic hands should provide a grip force of 45 N or more, a closing time of 0.8 s or less, and a weight of 500 g or less to offer the functions of normal activities in daily living [5]. Trade-offs exist between the actuation degree of freedom (DoF) for the dexterity, the grasping speed and force, and the weight of the robotic prosthetic hand; these mainly arise from the limited output of the actuator. Most robotic prosthetic hands employ geared electric motors such as DC or BLDC motors because they are compact and easily controlled, providing a better compromise solution than pneumatic and hydraulic actuators in small-to-medium-sized robotic systems. However, their maximum torque and permissible speed outputs are significantly bounded due to thermal, electric, and mechanical limitations, and they are not comparable with their human counterparts [6].

The control method of prosthetic hand systems has been another major challenge, and various control schemes have been proposed across prosthetic systems. First, commercial prosthetic hands adopt a direct on-off sequential control method. And studies on prosthetic hand control based on pattern recognition have been conducted [7], [8], and it has been shown to have high recognition accuracy and stability. Both approaches provide reliable control, but intuitive controls like a human hand are not possible because they use predefined grip patterns.

To implement intuitive control of the prosthetic hand, methods for the simultaneous proportional control (SPC) of fingers has been studied by estimating the relationship between the user's intention and electromyography (EMG) signals based on a model. There have been various studies that estimate the intention of finger movement or force in various ways, such as the linear matrix decomposition method [9], [10], the supervised learning method based on machine learning technology [11], and the semisupervised learning method [12].

Based on these element technologies, there have been efforts to integrate them into a single prosthetic system and verify the performance with human-involved experiments. Hahne, Janne M., *et al.* controlled two fingers simultaneously and proportionally based on linear regression (LR) and applied it to amputees to compare the results with previous methods [13]. In another study, an integration system of the prosthetic hand called Hannes

Manuscript received September 9, 2021; accepted December 16, 2021. Date of publication January 5, 2022; date of current version February 4, 2022. This letter was recommended for publication by Associate Editor Denny Oetomo and Editor Pietro Valdastrì upon evaluation of the reviewers' comments. This work was supported by the National Research Foundation of Korea (NRF) grant funded by the Korea government (MSIT) under Grant 2020R1A2B5B0200268912. (Corresponding author: Seokhwan Jeong; Kyung-Soo Kim.)

Younggeol Cho, Yeongseok Lee, and Kyung-Soo Kim are with the Department of Mechanical Engineering, Korea Advanced Institute of Science and Technology (KAIST), Daejeon 35226, South Korea (e-mail: younggeol-cho@kaist.ac.kr; yeongseok94@kaist.ac.kr; kyungsookim@kaist.ac.kr).

Pyungkang Kim is with the Samsung Electronics Co., Ltd, Hwasung 18448, South Korea (e-mail: kimpyungkang@gmail.com).

Seokhwan Jeong is with the Department of Mechanical Engineering, Sogang University, Seoul 04107, South Korea (e-mail: seokhwan@sogang.ac.kr).

This letter has supplementary downloadable material available at <https://doi.org/10.1109/LRA.2022.3140444>, provided by the authors.

Digital Object Identifier 10.1109/LRA.2022.3140444

was developed, and proportional grasping force control was performed [14]. In addition, there is a study used to control the prosthetic hand by determining the motion type of the hand based on muscle synergy and calculating the angle through the impedance model [8].

While there has been much research and progress in robotic prosthetic hand systems, control over the multiple DoFs of fingers in a proportional and simultaneous manner is still a challenging problem and remains in clinical research. To provide a more practical prosthetic hand platform, this letter presents a twofold solution consisting of the hardware and the software as a preliminary step integrating the prosthetic hand system. First, robotic prosthetic hand hardware using a novel actuation mechanism, called a 2-speed twisted string actuator (TSA) [15], is presented. The actuation mechanism has a two-stage transmission ratio so that the prosthetic hardware can produce a high grasping force in force mode or a fast grasping speed in speed mode while maintaining a light weight, satisfying the prosthesis's performance criterion. Second, a new intention estimation model based on electromyography was applied to prosthetic control, and the performance was verified through standardized experiments and demonstrations.

From the hardware and the software improvements developed in this work, the contributions of this letter can be summarized as follows:

- 1) All the actuation mechanisms were integrated into a single module to offer an independent and highly portable actuator module.
- 2) The prosthetic robot hand hardware satisfying the minimum grasping performance requirement is presented.
- 3) The EMG acquisition circuit includes a Right Leg Driver (RLD) that actively reduces common noise, and the bulky circuit is embedded in the PCB and shielded to improve the signal quality and measure a robust EMG signal.
- 4) The number of channels was reduced, and the neural network structure was simplified to enable operation in the limited MCU computing power of the integrated prosthetic system.
- 5) All above element technologies are integrated into a single prosthetic system with high portability.

II. THE MSC PROSTHETIC HAND

Fig. 1 shows the developed MSC prosthetic robot hand system. The MSC prosthetic hand system is composed of robotic hardware, an sEMG signal acquisition part, and a portable electronic board including motor drivers and a microprocessor for controller and data processing. This section presents the design and working principle of each part and the integration procedure underlying the prosthetic hand system.

A. Hardware of MSC Prosthetic Hand

The developed MSC prosthetic hand (see Fig. 2) is a design iteration of the previous versions of robotic hands [22], [23]; the hardware consists of actuators, sensors, and a hand frame including five fingers, which provide a gateway for an amputee to interact with the physical world. While the overall hand frame

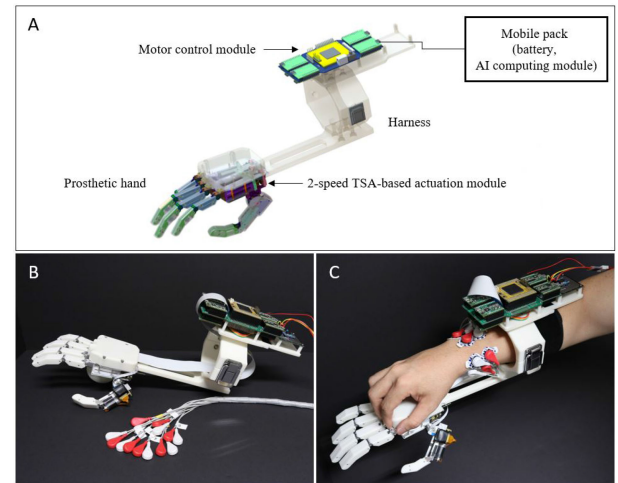


Fig. 1. The MSC prosthetic hand. A. Rendered image of the integrated system. B. Appearance of the prosthetic hand including integrated board and harness. C. Wearing the prosthesis on the arm.

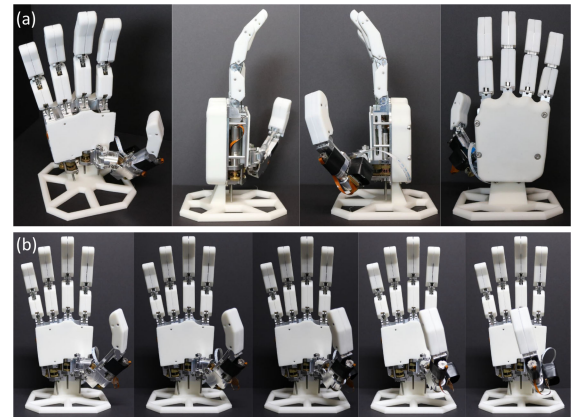


Fig. 2. (a) Developed MSC prosthetic hand. (b) Passive abduction/adduction motion of the thumb.

has the same structure as previous frames, we have made several modifications to the actuation mechanism and finger design.

Most conventional prosthetic robot hands [5] employ electric motors (e.g., DC/BLDC motors) providing a single transmission ratio mechanisms (e.g., spur/bevel gears with a fixed gear ratio), but the conventional actuation mechanisms cannot achieve the speed and force of a human hand due to the limited speed/torque operational range of the electric motors. Therefore, conventional prosthetic robot hands provide a compromised range of outputs that trade off between speed and torque and cannot achieve the grasping performance of a human hand (see Table I). Belter [5] reviewed performance guidelines for the prosthetic hands; a grip force (i.e., pinch force or fingertip force) greater than 45 N [24] and a grasping speed (i.e., closing time) less than 0.8s [25] were proposed as design requirements to support the normal activities of daily living and practical use.

To overcome the narrow output range of electric motors and satisfy the minimum grasping performance requirement, in this work, we developed a new modular design of 2-speed TSA-based compact transmission mechanism, whose initial

TABLE I
PERFORMANCE OF PROSTHETIC ROBOT HANDS

Items	Pinch force (Power grasping) (N)	Closing time (s)	Weight (g)	DOF	Ref.
i-Limb Ultra Flexion	21	0.8	628	6	[16]
Bebionic Hand	26.5	1	591	5 + 1(passive)	[17]
Michelangelo	70	1	460	2	[18]
Modular Prosthetic Limb	66.7	0.3	1315	12	[19]
Luke Arm (Radial)	-	0.3-0.5	1400	8	[20]
DMC hand	- (90)	0.6	355	1+1(wrist)	[21]
Hannes Hand Prosthesis	- (150)	0.8	480	1	[14]
Proposed MSC Prosthetic Hand	45(force mode)	0.5(speed mode)	390	4+1(passive)	

TABLE II
THE PERFORMANCE INDICES OF THE TARGET REACHING EXPERIMENT

Performance Indices	Explanation
Completion rate (α , [%])	The number of completed trials / Total trials
Completion time (t_c , [s])	The time to complete a trial
Overshoots (k)	The number of red bar crosses the target
Efficiency coef (Γ , [%])	Optimal trajectory length / Actual trajectory length

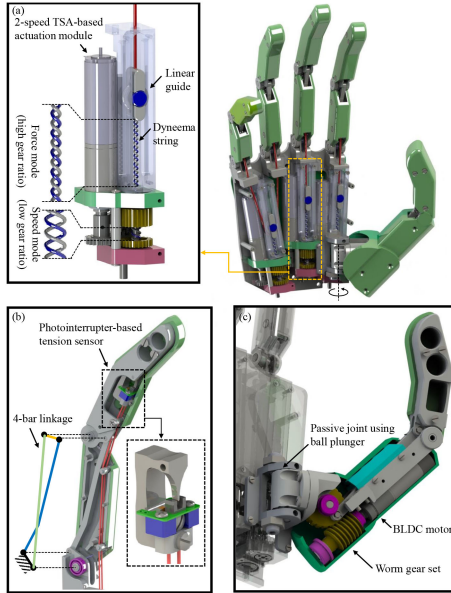


Fig. 3. Schematic of the MSC prosthetic hand. (a) 2-speed TSA-based actuation module. (b) Finger design and photointerrupter-based tension sensor. (c) Thumb design with the manual joint.

concept was introduced in [15], as the actuator of the MSC prosthetic hand (see Fig. 3(a)). The transmission mechanism can selectively choose two different operational modes (i.e., speed mode: low transmission ratio, force mode: high transmission ratio) providing different twisted radii, which gives the actuation module 2-speed variable transmission ratios. This mechanism allows the actuation module to have a very compact size (i.e., 20.7mm×20.7mm×58.6mm) compared to conventional variable transmission mechanisms. In this work, all mechanical parts, the twisted strings, and BLDC motors (i.e., main motor (8 W, 315170, Maxonmotor) and clutch motor (2 W, 455419, Maxonmotor)) were integrated into a single module to offer an independent and highly portable actuator module; and three

actuation modules were embedded in the footprint of the hand. This actuation mechanism allows the developed prosthetic robot hand to have an average fingertip force of 45 N overall for grasping postures in the force mode (under stall torque conditions) and a 0.5s closing time in the speed mode. Considering the actuated DoFs and weight, we believe that the performance is outstanding compared to the existing systems (see. Table I) and fully satisfies the proposed performance criteria for both speed and force simultaneously. The supplementary video 2 (Video S2) shows a grasping demonstration in the each operation mode.

Considering the independence of human fingers [26], each index and middle finger of the MSC prosthetic was designed to have one actuation DoF to increase grasping dexterity. The ring and little finger share a single actuation module using a tendon-based differential mechanism considering human finger correlations [26]. Due to the important role of thumb movements in grasping [27], [28], the thumb was designed to provide two DoFs: flexion/extension (FE) and abduction/adduction (AA) motion (see Fig. 3(c)). A compact BLDC motor (8 W, 315173, Maxonmotor) and a worm gear transmission embedded in the thumb generate AA motion. The non-backdrivable feature of the worm gear set allows the thumb to support an object as a counterpart of the fingers from the index to the little. To provide various opposition postures for the thumb, AA motion is implemented with a passive adjustment of the ball plunger so that the user can choose different AA postures up to 120 degrees (e.g., palmar or radial AA) by changing its orientation (see Fig. 3(c) and Fig. 2(b)). The proximal interphalangeal (PIP) and metacarpophalangeal (MCP) joints of the index to the little finger and the metacarpophalangeal and carpometacarpal joints of the thumb are coupled with 4-bar linkages in the same way as previous versions.

The MSC prosthetic can use either position- or force-based control methods; therefore, we embedded a customized optic-based compact force sensor [29] at the tip of the finger to measure the tendon tension and control the grasping force.

B. Integration System Details: Myoelectric Modules and Controller

The electric part of the MSC hand control using EMG is composed of a motor control module and a signal acquisition/AI computing module (see. Fig. 4). The communication between modules used a controller area network (CAN).

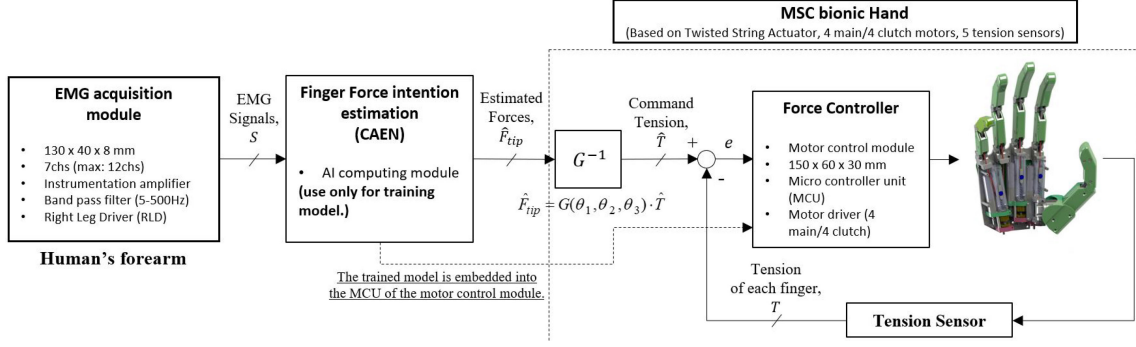


Fig. 4. Closed loop schematic diagram of the proposed integrated system including motor control module and signal acquisition/AI computing module.

The motor control module includes a motor driver (ESCON module 24/2) for driving the TSA module and a microcontroller unit (MCU; TMS320F28379D, Texas Instruments) for processing input/output signals and embedding the controller. The motor driver has a built-in current controller for the motor mounted on the MSC prosthetic hand and receives the control input from the MCU. The MCU receives information from the hall sensor mounted on the BLDC motor of the actuation module and the small tension sensor mounted to the fingertip. The MCU was programmed to control the operational mode (i.e., transmission ratio) of the actuation modules, and its controller was configured based on a simple PID and disturbance observer (DOB) with measure of the string tension (or grasping force). Additionally, through feedback control of the clutch gear position, accurate and stable switching between the speed mode and force mode can be achieved.

For EMG signal acquisition and processing, we developed a module containing a circuit and MCU for signal amplification and noise removal. It is of a sufficiently compact size (i.e., 60 mm × 140 mm × 25 mm) to be built into the arm harness and is designed to process up to 12 channels of signals. A differential amplifier (INA 128, Texas Instruments) and a right leg driver (RLD) were designed to reject external electrical interference and common noise. Seven-channel disposable electrodes (ECG Electrodes, Ag/AgCl, Kendall) were attached to the wrist except for the radius and ulna to obtain an EMG signal, and then a 5-500 Hz secondary bandpass filter was applied. The filter was used to selectively acquire the main frequencies of the EMG. Afterwards, the second order IIR Butterworth bandpass filter and notch filter of the same frequency as the analog filter were applied to the EMG acquired through the ADC of the MCU. The finger force intention was estimated by calculating the CAEN model from the processed EMG digital signal in the AI computing module. Jetson Xavier NX (NVIDIA) was used as the AI computing module, and the software was developed using ROS and C++. By enabling EMG signal monitoring, training of the intention estimation model, and real-time estimation of finger force using the model, a portable integrated prosthetic system that does not require additional equipment was established. The AI computing module is used only for training, and only the MCU in the motor control module is used for prosthetic operation.

III. MYOELECTRIC CONTROL OF THE PROSTHETIC HAND

A. Real-Time Finger Force Intention Estimation

The purpose of this study is to intuitively control the prosthetic hand by estimating the intention of the user's finger simultaneously and proportionally using the electromyography. Unlike the method that uses the pattern recognition technique to determine several grip types and select the control sequence, the proposed method is a regression-based method similar to the method of moving a human hand. Therefore, it is possible to intuitively control the finger force of the prosthetic hand through the proposed model without a discrete grip pattern and a method of adjusting it in order in advance. The finger force intent was estimated using constrained autoencoder (CAEN) based on multichannel EMG signals. CAEN is a new semi-supervised intention estimation model proposed by this research group [30]. The model is trained to maximize the independence between the fingers, and it is possible to simultaneously and proportionally estimate the intention of the finger force. In previous studies, CAEN showed high performance in intention estimation accuracy and interfinger independence compared to the SPC model of the preceding regression method. The performance was also verified through virtual real-time prosthetic control simulation. The detailed CAEN model and verification results are shown in [30]. Based on the previous study, the number of channels was reduced for system embedding, and the structure of the neural network was simplified. In addition, a robust signal was obtained by developing a compact PCB-type module including a Right Leg Driver (RLD) from the previous bulky circuit. As a result, the amount of computation for intention estimation was reduced to 12%, and the accuracy of intention estimation was improved through robust signal acquisition. The CAEN model consists of five layers with a left-right symmetric structure, and the node in the middle hidden layer represents the estimated value of the intention of each finger force. The forward calculation process is as follows.

$$\hat{F} = f_2(W_2 * f_1(W_1 * S + b_1) + b_2) \quad (1)$$

$$S' = W_4 * f_1(W_3 * \hat{F} + b_3) + b_4 \quad (2)$$

The input layer value of the EMG signal ($S \in R^{N \times T}$) is encoded with weights (W_1, W_2), bias (b_1, b_2), and activation functions

$(f_1), f_2)$, and the node value of the intention estimation layer, \hat{F} , is calculated. For f_1 and f_2 , a rectified linear unit (RELU) and a hyperbolic tangent function (tanh) were used, respectively. Similarly, the output layer S' was calculated through decoding weights (W_3, W_4) and bias (b_3, b_4). The cost function (J) for CAEN model training was defined as the sum of two cost functions with different objectives. One objective is to make the input layer (S) and the output layer (S') the same, and the other objective is to estimate the finger force intent while simultaneously maximizing the independence between the fingers.

$$J = \|S - S'\|_2 + \frac{\|(1 - C) * (\hat{F} \circ \hat{F})\|_2}{\|C * (\hat{F} \circ \hat{F})\|_2} \quad (3)$$

The cost function includes a constraint matrix C representing the on/off of the finger that applies force when acquiring data for modeling. C is a matrix in which the column corresponding to the applied finger is 1, and the remainder is 0. An example is as follows.

$$C = \begin{bmatrix} C_{T,t_1} & C_{T,t_2} & C_{T,t_3} & \dots \\ C_{I,t_1} & C_{I,t_2} & C_{I,t_3} & \dots \\ C_{M,t_1} & C_{M,t_2} & C_{M,t_3} & \dots \end{bmatrix} = \begin{bmatrix} 1 & 0 & 0 & \dots \\ 0 & 1 & 0 & \dots \\ 0 & 0 & 1 & \dots \end{bmatrix} \quad (4)$$

Consequently, by minimizing the cost function, the model is trained to estimate the finger force intent and maximize the independence between fingers.

B. Prosthetic Hand Control Based on Estimated Finger Force Intention

The finger force intent estimated using CAEN is normalized from 0 to 1 based on the maximum value. In addition, in this study, since the finger intentions of three degrees of freedom (thumb, index, middle finger) were estimated, the ring and little fingers were operated together as the control input of the middle finger. The finger force intent estimate was mapped to the angle of each finger of the prosthetic hand. To secure the control stability of the prosthetic hand, it was operated when the finger force intention value was 0.2 or more, and when the intention value was 1 or more, it was maintained at 1. In addition, a moving average filter was applied to the prosthetic hand control input to prevent prosthetic control instability due to sudden changes in EMG prompted by external electrical interference and muscle tremors.

IV. EXPERIMENTAL DETAILS

A. Subjects

Five healthy subjects (23–38 a old) and one subject with amputation (40 a old) participated in this experiment. All healthy subjects had intact hand function and no history of hand-related disease. All experiments were conducted with the dominant hand, and institutional approval was obtained from the KAIST Institutional Review Board (IRB No.KH2018-95).

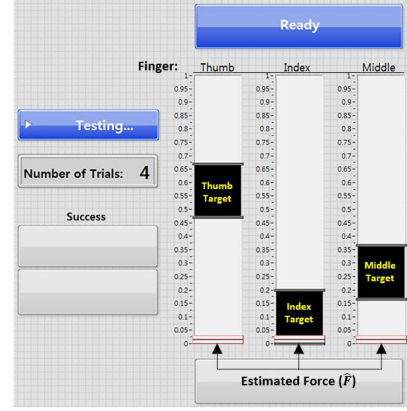


Fig. 5. The target reaching experiment (TRE).

B. Performance Validation of the Finger Force Intention Estimation

To verify the performance of the intention estimation model applied to the prosthetic hand, the difference between the finger force intention estimated by electromyography (\hat{F}) and the force measured using a load cell attached to the fingertip (\bar{F}) was analyzed. The difference between the two values is defined as the normalized root mean square error (NRMSE), and the formula is as follows.

$$NRMSE = \|F - \hat{F}\|_2 \quad (5)$$

All cases where each finger moved individually and simultaneously at 3 degrees of freedom (DOF) were analyzed. Experiments were performed 5 times in each case of applying force to each finger, and thus 35 sets of experimental results were analyzed per subject.

C. Online Simulation: Target Reaching Experiment

We performed a target reaching experiment (TRE), a real-time simulation to test prosthetic control performance, citing previous studies [30], [31]. TRE is an experiment performed with visual feedback. The finger force estimated through the model is expressed as the position of the bar on the monitor, and the bar reaches the target at a specific position (see. Fig. 5). The bar was allowed to move between zero and one by inputting a normalized estimated force, and the target was selected as 20% of the total travel path. Participants performed a total of thirty-five different target positions, and the time limit for each problem was set to 20 seconds. We placed the target in missions to reflect all areas. The TRE performance indicators were selected from the four cited in previous letters (see. Table II).

D. Box and blocks Test

The box and blocks test (BBT) is a standardized method for evaluating manual dexterity and is being used to evaluate the performance of the prosthetic hand [32]. This is a test of moving blocks from one side to the other of wooden box sized 53.7 cm×25.4 cm×8.5 cm and with a 15.2 cm partition. The block is a cube with each edge 2.5 cm long, and all blocks

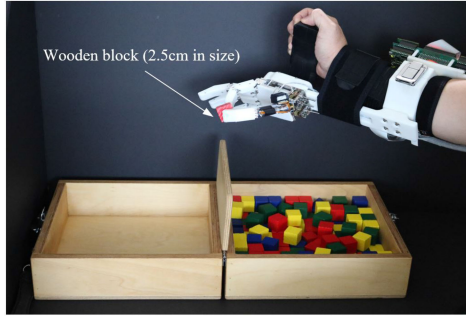


Fig. 6. The box and block test (BBT).

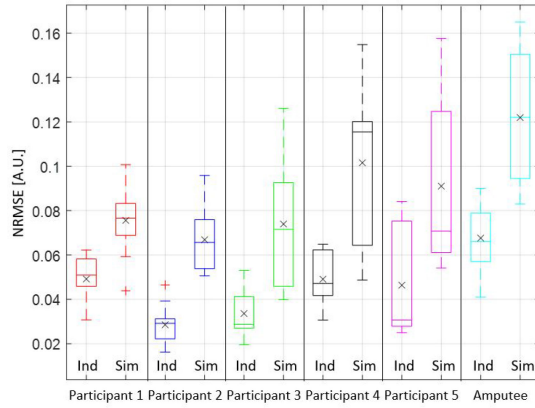


Fig. 7. Performance of the finger force intention estimation, which is the result from estimating individual (Ind) and simultaneous (sim) finger forces. Average (x symbol), max, and min values are shown. In addition, 25% and 75% values are displayed through the error bar. The mean value of NRMSE for all people is 0.067.

have the same weight. Precise control of the prosthetic hand is essential because the force of the two fingers must be the same and in an appropriate position to hold the block. Additionally, to approach the block, the shoulder and elbow joints must be moved, so EMG changes can occur at this time. Therefore, a high score can be obtained only when stable intention estimation is possible.

The BBT equipment is represented in Fig. 6. The experimental process measures the number of blocks moved over 1 minute after 15 seconds of practice time. In this study, each subject was tested 5 times, and the evaluation index was selected as the average time it took to move each block over 1 minute.

V. RESULTS

A. Performance of Finger Force Intention Estimation

The results from analyzing the difference between the measured force and the force estimated through the intention estimation model are as follows (see Fig. 7). The average across the 5 healthy participants showed an error of approximately 4% compared to the measured force when applying force to each finger separately. When applying simultaneous finger force, there was an error of approximately 8%. In the case of the subject with amputation, individual and simultaneous finger estimation showed errors of 6.7% and 12.1%, respectively. In a previous

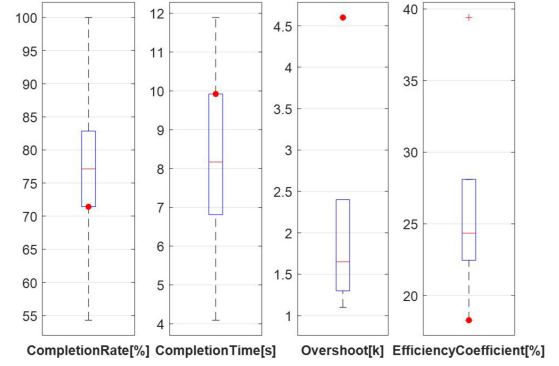


Fig. 8. Target Reach Experiment Results. Statistical values of healthy subjects according to each performance index are shown, and red dots are results of subject with amputation.

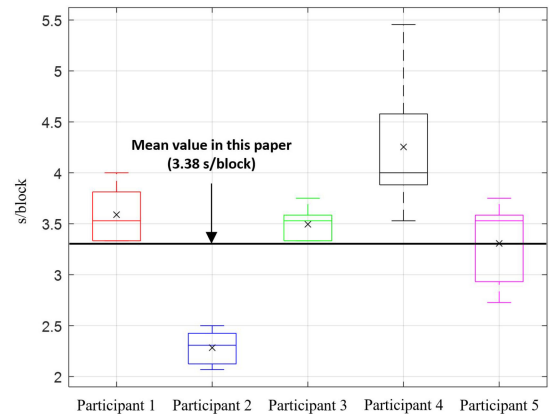


Fig. 9. Result of the BBT. The average value is 3.38 s/block. Among the 5 participants, the fastest result was 2.06 s/block (29 blocks), and the slowest result was 5.45 s/block (11 blocks).

study [30], a detailed performance comparison of CAEN and previous intention estimation methods was performed, and high model accuracy and real-time simulation considering the prosthetic control situation showed high performance.

B. Performance of the Online Simulation

The online simulation results in which humans were included in the control loop are as follows (see Fig. 8). The average results of healthy participants were 78% success rate, 7.82 s success time, 1.6 overshoot, and 27% trajectory. The subject with amputation showed 71% success rate, 9.92 s success time, 4.6 overshoot, and 18% trajectory efficiency. In the result of the subject with amputation, the success rate and success time showed performance indicators within the statistical boundaries of healthy subjects, but the overshoot and trajectory efficiency were low. This is analyzed because the forearm muscle was not used after amputation, and the muscle degenerated and the EMG tremor was severe. In addition to these results, a detailed performance comparison of CAEN in the target reaching experiment was performed in a previous study [30]. Ten healthy subjects participated in the experiment and showed superior performance compared to the previous model.

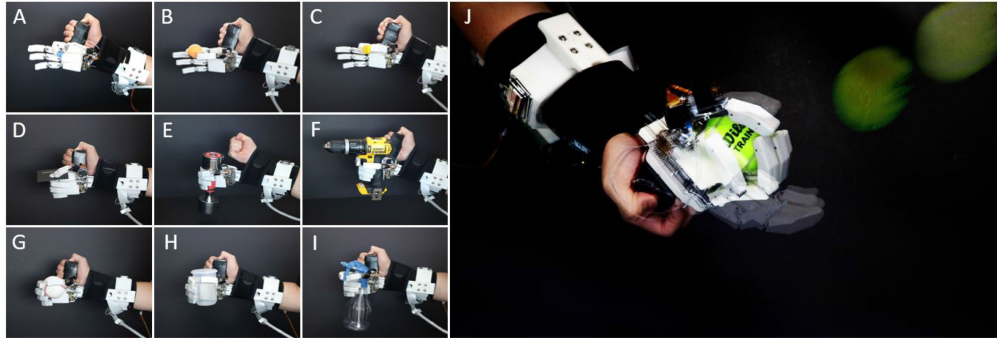


Fig. 10. Demonstration. Precision grasp (A. bead, B. ping-pong balls, C: block), Lateral grasp (D. business card), Power grasp (E. dumbbell, F. drill), etc (G. baseball, H. plastic cup, I. spray gun). and J. Catch ball experiment showing that high-speed gripping is possible.

C. Results From Box and Blocks Test

The results of the 5 subjects' BBT experiments are shown in Fig. 9. The time per block is distributed from a minimum of 2.06 s/block to a maximum 5.45 s/block, and the average value is 3.38 s/block. To the best of our knowledge, 5 participants performed BBT in a recent study published examining state of the art upper limb prostheses [13], and the results showed superior values in the performance index compared to the results of the previous study. However, since the previous study was the result of subject with amputation, only indirect comparison is possible.

VI. DISCUSSION

When demonstrating to show the function of MSC hand prostheses, we conducted an experiment to pick up a total of 9 objects that are common in daily life. as shown in Fig. 10(A, B, C), precision grasping was demonstrated by picking up small spherical objects (beads, ping-pong balls) and cubes (blocks). We showed examples of lateral grasping (Fig. 10 (D)) through picking up a business cards using thumbs and index fingers, and power grasping by lifting a 3 kg dumbbell and a 5 kg drill (Fig. 10(E, F)). In addition, it was confirmed that different types of objects such as baseball, plastic cup, and spray gun (Fig. 10(G, H, I)) can be picked up. Since the prosthetic hand developed in this study has a fast grasping speed in speed mode, and real-time finger force intention estimation is possible, it is possible for the user of the prosthesis to grasp rapidly in intuitive manner. To demonstrate this, we conducted a demonstration of a situation that requires a quick grasp, throwing a ball. The experiment showed that it is possible to catch a ball flying at a high speed using the hand as shown in Fig. 10(J), in a form similar to that before amputation. A demonstration video is shown in Video S1

The prosthetic hand presented in this study was developed with a fixed wrist. Therefore, for hand rotation, wrist movement had to be replaced with shoulder and elbow rotation. To develop a more human-like upper limb prosthesis, the hardware development of the wrist and the algorithm for moving it should be studied together, and previous studies have shown the possibility of estimating wrist intention [33].

Since the operating mode (i.e., speed/force modes) of the 2-speed TSA actuation module was manually controlled in this work, it is necessary to develop a high-level control algorithm for active switching between the two transmission ratios to facilitate the full function of the variable transmission ratio, which may

provide a human-level grasping function. The EMG signal or the external interacting force measured by the tension sensor embedded at the fingertip can be used as a threshold value of the mode switching.

In a previous study [13] that compared BBT results, an experiment was performed with a 2-DOF intention estimation model, but in this study, a 3-DOF (T, I, M finger) model was used. In other words, it is expected that tasks can be performed through various finger movements. However, since the participants in this study were able-bodied and the results were for subjects with amputations, direct comparison was difficult. Previous studies [34] have mentioned the characteristics of the EMG change in time and frequency after the amputation of the hand. Therefore, an experimental validation of the prosthesis developed in this study for subject with amputations should be conducted in the future.

In addition to the development of the high-performance prosthetic arm shown in this study and intuitive and accurate prosthetic control, it is essential to study the feedback of the user's senses. In previous studies, a method of feedback the grasping force or slip of the prosthetic hand has been proposed [35], [36], and it has been verified that the prosthetic hand control performance is improved. Additionally, we proposed a sensory feedback method [37] using mixed-modality stimulation in a previous letter. Based on this, research applied to the prosthesis is in progress, and we plan to show a study on a closed loop prosthetic integrated system including sensory feedback in the future.

In this study, five healthy subjects and one subject with amputation participated in the experiment. Statistical analysis will be carried out through experiments by a number of subjects with amputation in the future, and the results of amputee in this study showed the potential as a case study.

VII. CONCLUSION

In this study, the hardware and control algorithm of the MSC prosthetic hand were introduced and its performance was verified by applying it to humans. We developed a new prosthetic hand to which a TSA-based 2-speed transmission ratio actuation is applied and controlled it with an AI-based finger force intention estimation algorithm using electromyography. The developed prosthetic hand has the distinctive feature of dual mode, and it was able to secure fast grasping speed and high force in each mode. In addition, a very light prosthetic hand (390 g) was developed by applying TSA, which has high

weight-efficiency. In addition, a portable system was developed by establishing an integrated system including electric field units and software for EMG acquisition, AI training, and calculation. The performance of the developed prosthesis was verified through a standardized experiment called the box and blocks test and by demonstrating the grasping of various objects. As a result of the BBT, the participants succeeded in holding the block by controlling the two fingers to an appropriate position with the same force, and showed a higher performance index value compared to the previous study. This was made possible by the combination of the high estimation accuracy of the finger intention estimation model, the structural design of the prosthetic hand, and the precise control of the twist actuator. In a future study, the performance of the prosthetic hand will be verified on an subject with amputation, and a study on the rehabilitation process to help the user adapt will be conducted. In addition to the experiments performed in this study, the prosthetic hand will be improved by conducting experiments that reflect more real-life work performance. Finally, we will conduct research with the goal of putting the developed prosthetic hand into practical use.

REFERENCES

- [1] D. Farina *et al.*, "Toward higher-performance bionic limbs for wider clinical use," *Nature Biomed. Eng.*, pp. 1–13, 2021.
- [2] D. Farina and S. Amsüss, "Reflections on the present and future of upper limb prostheses," *Expert Rev. Med. Devices*, vol. 13, no. 4, pp. 321–324, 2016.
- [3] F. Cordella *et al.*, "Literature review on needs of upper limb prosthesis users," *Front. Neurosci.*, vol. 10, no. 209, pp. 1–14, 2016.
- [4] E. A. Biddiss and T. T. Chau, "Upper limb prosthesis use and abandonment: A survey of the last 25 years," *Prosthetics Orthotics Int.*, vol. 31, no. 3, pp. 236–257, 2007.
- [5] J. T. Belter *et al.*, "Mechanical design and performance specifications of anthropomorphic prosthetic hands: A review," *J. Rehabil. Res. Develop.*, vol. 50, no. 5, pp. 599–618, 2013.
- [6] J. Huber, N. Fleck, and M. Ashby, "The selection of mechanical actuators based on performance indices," *Proc. Roy. Soc. London. Ser. A: Math., Phys. Eng. Sci.*, vol. 453, no. 1965, pp. 2185–2205, 1997.
- [7] M. Tavakoli, C. Benussi, P. A. Lopes, L. B. Osorio, and A. T. de Almeida, "Robust hand gesture recognition with a double channel surface EMG wearable armband and SVM classifier," *Biomed. Signal Process. Control*, vol. 46, pp. 121–130, 2018.
- [8] A. Furui *et al.*, "A myoelectric prosthetic hand with muscle synergy-based motion determination and impedance model-based biomimetic control," *Sci. Robot.*, vol. 4, no. 31, pp. 1–12, 2019.
- [9] L. H. Smith, T. A. Kuiken, and L. J. Hargrove, "Evaluation of linear regression simultaneous myoelectric control using intramuscular EMG," *IEEE Trans. Biomed. Eng.*, vol. 63, no. 4, pp. 737–746, Apr. 2016.
- [10] N. Jiang, H. Rehbaum, I. Vujaklija, B. Graimann, and D. Farina, "Intuitive, online, simultaneous, and proportional myoelectric control over two degrees-of-freedom in upper limb amputees," *IEEE Trans. Neural Syst. Rehabil. Eng.*, vol. 22, no. 3, pp. 501–510, May 2014.
- [11] J. L. Nielsen, S. Holmgard, N. Jiang, K. B. Englehart, D. Farina, and P. A. Parker, "Simultaneous and proportional force estimation for multifunction myoelectric prostheses using mirrored bilateral training," *IEEE Trans. Biomed. Eng.*, vol. 58, no. 3, pp. 681–688, Mar. 2011.
- [12] P. Kim, K.-S. Kim, and S. Kim, "Modified nonnegative matrix factorization using the hadamard product to estimate real-time continuous finger-motion intentions," *IEEE Trans. Hum.-Mach. Syst.*, vol. 47, no. 6, pp. 1089–1099, Dec. 2017.
- [13] J. M. Hahne, M. A. Schweisfurth, M. Koppe, and D. Farina, "Simultaneous control of multiple functions of bionic hand prostheses: Performance and robustness in end users," *Sci. Robot.*, vol. 3, no. 19, 2018, Art. no. eaat3630.
- [14] M. Laffranchi *et al.*, "The hannes hand prosthesis replicates the key biological properties of the human hand," *Sci. Robot.*, vol. 5, no. 46, pp. 1–15, 2020.
- [15] S. H. Jeong and K.-S. Kim, "A 2-speed small transmission mechanism based on twisted string actuation and a dog clutch," *IEEE Robot. Automat. Lett.*, vol. 3, no. 3, pp. 1338–1345, Jul. 2018.
- [16] OSSUR, "i-limb ultra flexion," Accessed: Sep. 09, 2021. [Online]. Available: <https://www.ossur.com/en-us/prosthetics/arms/i-limb-ultra-titanium>
- [17] ottobock, "Bebionic v3," Accessed: Sep. 09, 2021. [Online]. Available: <https://www.ottobockus.com/prosthetics/upper-limb-prosthetics/solution-overview/bebionic-hand/>
- [18] ottobock, "Michelangelo," Accessed: Sep. 09, 2021. [Online]. Available: <https://www.ottobockus.com/prosthetics/upper-limb-prosthetics/solution-overview/michelangelo-prosthetic-hand/>
- [19] J. Hopkins, "Modular prosthetic limb," Accessed: Sep. 09, 2021. [Online]. Available: <https://www.jhuapl.edu/Prosthetics/ResearchMPL>
- [20] MOBIUS bionics, "Luke arm (radial)," Accessed: Sep. 09, 2021. [Online]. Available: <https://www.mobiusbionics.com/luke-arm/>
- [21] ottobock, "DMC hand," Accessed: Sep. 09, 2021. [Online]. Available: https://shop.ottobock.us/Prosthetics/Upper-Limb-Prosthetics/Myo-Hands-and-Components/Myo-Terminal-Devices/System-Electric-Hand-DMC-Plus/p/8E38_56#product-documents-section
- [22] S. H. Jeong, K.-S. Kim, and S. Kim, "Designing anthropomorphic robot hand with active dual-mode twisted string actuation mechanism and tiny tension sensors," *IEEE Robot. Automat. Lett.*, vol. 2, no. 3, pp. 1571–1578, Jul. 2017.
- [23] S. Jeong, Y. Lee, and K.-S. Kim, "Applications: Twisted string actuation-based compact automatic transmission," in *Proc. IEEE Int. Conf. Robot. Automat.*, 2021, pp. 10870–10876.
- [24] R. Vinet *et al.*, "Design methodology for a multifunctional hand prosthesis," *J. Rehabil. Res. Develop.*, vol. 32, no. 4, pp. 316–324, 1995.
- [25] A. Tözeren, *Human Body Dynamics: Classical Mechanics and Human Movement*. Springer Science & Business Media, 1999.
- [26] J. N. Ingram, K. P. Kording, I. S. Howard, and D. M. Wolpert, "The statistics of natural hand movements," *Exp. Brain Res.*, vol. 188, no. 2, pp. 223–236, 2008.
- [27] G. Cotugno, K. Althoefer, and T. Nanayakkara, "The role of the thumb: Study of finger motion in grasping and reachability space in human and robotic hands," *IEEE Trans. Syst., Man, Cybern. Syst.*, vol. 47, no. 7, pp. 1061–1070, Jul. 2017.
- [28] D. L. Hart, S. J. Isernhagen, and L. N. Matheson, "Guidelines for functional capacity evaluation of people with medical conditions," *J. Orthopaedic Sports Phys. Ther.*, vol. 18, no. 6, pp. 682–686, 1993.
- [29] S. H. Jeong, H. J. Lee, K.-R. Kim, and K.-S. Kim, "Design of a miniature force sensor based on photointerrupter for robotic hand," *Sensors Actuators A: Phys.*, vol. 269, pp. 444–453, 2018.
- [30] Y. Cho, P. Kim, and K.-S. Kim, "Estimating simultaneous and proportional finger force intention based on sEMG using a constrained autoencoder," *IEEE Access*, vol. 8, pp. 138264–138276, 2020.
- [31] N. Jiang, I. Vujaklija, H. Rehbaum, B. Graimann, and D. Farina, "Is accurate mapping of EMG signals on kinematics needed for precise online myoelectric control?" *IEEE Trans. Neural Syst. Rehabil. Eng.*, vol. 22, no. 3, pp. 549–558, May 2014.
- [32] V. Mathiowetz, G. Volland, N. Kashman, and K. Weber, "Adult norms for the box and block test of manual dexterity," *Amer. J. Occup. Ther.*, vol. 39, no. 6, pp. 386–391, 1985.
- [33] Y. Cho, P. Kim, and K.-S. Kim, "Electrical impedance myography (EIM) for multi-class prosthetic robot hand control," in *Proc. 20th Int. Conf. Control, Automat. Syst.*, 2020, pp. 1092–1094.
- [34] E. Campbell, A. Phinyomark, A. H. Al-Timemy, R. N. Khushaba, G. Petri, and E. Scheme, "Differences in EMG feature space between able-bodied and amputee subjects for myoelectric control," in *Proc. 9th Int. IEEE/EMBS Conf. Neural Eng.*, 2019, pp. 33–36.
- [35] N. Jorgovanovic, S. Dosen, D. J. Djovic, G. Krajcoski, and D. Farina, "Virtual grasping: Closed-loop force control using electrotactile feedback," *Comput. Math. Methods Med.*, vol. 2014, pp. 1–13, 2014.
- [36] D. D. Damian, A. H. Arita, H. Martinez, and R. Pfeifer, "Slip speed feedback for grip force control," *IEEE Trans. Biomed. Eng.*, vol. 59, no. 8, pp. 2200–2210, Aug. 2012.
- [37] K. Choi, P. Kim, K.-S. Kim, and S. Kim, "Mixed-modality stimulation to evoke two modalities simultaneously in one channel for electrocutaneous sensory feedback," *IEEE Trans. Neural Syst. Rehabil. Eng.*, vol. 25, no. 12, pp. 2258–2269, Dec. 2017.